Alamethicin Incorporation in Lipid Bilayers: A Thermodynamic Study†

Vincenzo Rizzo, Stefan Stankowski, and Gerhard Schwarz*
Department of Biophysical Chemistry, Biocenter of the University of Basel, CH-4056 Basel, Switzerland
Received July 23, 1986; Revised Manuscript Received December 8, 1986

ABSTRACT: Interaction of the peptide antibiotic alamethicin with phospholipid vesicles has been monitored by changes in its circular dichroic and fluorescent properties. The data are consistent with an incorporation of the peptide in the lipid bilayer. Aggregation of alamethicin in the membrane phase is evident from a characteristic concentration dependence of the incorporation, reflecting the existence of a critical concentration. The data can be fully understood in terms of a theoretical approach that includes aggregation and thermodynamic nonideality. Thermodynamic parameters of the peptide–lipid interaction have been evaluated under a variety of conditions of temperature, ionic strength, and lipid type (saturated and unsaturated fatty acid chains). From the results obtained in this study, one can extrapolate to the incorporation behavior of alamethicin at low concentrations, as they are typical for measurements of conductance across planar lipid films. This leads to a simple explanation of the voltage-gating mechanism of alamethicin in a straightforward way.

Alamethicin, a natural peptide produced by the fungus *Trichoderma viride*, has been the subject of numerous investigations for its ability to induce voltage-gated conductance in black lipid membranes (Gordon & Haydon, 1975; Eisenberg et al., 1973; Boheim & Kolb, 1978; Latorre & Alvarez, 1981). Because of this striking analogy with the properties of much more complex membrane proteins, alamethicin is considered a model for voltage-gated ion channels (Hall et al., 1984). The elucidation of the molecular details for alamethicin activity in membranes may thus contribute to advancing our knowledge of important biological functions.

The determination of the correct sequence (Rinehart et al., 1977) and of the crystal structure (Fox & Richards, 1982), together with a variety of studies in solution (Nagaraj & Balaram, 1981; Jung et al., 1975; Banerjee et al., 1983), has greatly contributed to establishing the current picture of alamethicin as an amphipathic molecule favoring a largely helical conformation in nonpolar environments. Black lipid film studies indicate that aggregates are responsible for the conducting states in the membrane and set the number of peptide molecules in a pore to an average of about 8–10 (Boheim, 1974). Aggregation is also observed both in aqueous solution (McMullen & Stirrup, 1979) and in organic solvents (Schwarz & Savko, 1982). This property appears to be a natural consequence of the amphipathic characteristics of alamethicin (Mathew & Balaram, 1983a,b; Fox & Richards, 1982).

Physicochemical investigations of the interaction between alamethicin and lipid bilayers may provide the necessary link between functional studies in the membrane and structural studies in solution or in the solid state. In our opinion, this issue has not been adequately pursued in the literature. Therefore, we have undertaken an extensive thermodynamic and kinetic analysis of alamethicin incorporation into lipid bilayers. In this paper we present and discuss thermodynamic data obtained with two different lipids (DMPC[1] and DOPC) under a variety of conditions (temperature, ionic strength). An investigation of the kinetic aspects is in progress.

The data collected so far are consistent with an insertion of the molecule into the aliphatic core of the bilayers even in the absence of an electric potential. The same conclusion had been reached before by Latorre et al. (1981), using chemical cross-linking experiments. This mode of interaction, which we refer to as incorporation, can be treated as a solution process of the peptide (the solute) in the lipid (the solvent). In a previous paper (Schwarz et al., 1986) we developed a suitable thermodynamic treatment, including nonideal effects due to the high concentration that can be obtained by alamethicin in bilayers. The main results of this treatment, as summarized under Materials and Methods, have been used in the analysis of data presented here. Considerable care in the evaluation of experimental results was required because of the clearly detectable alamethicin aggregation in the lipid phase. In particular, we use a novel approach for the determination of spectroscopic parameters of the incorporated form. This approach may be also of importance for the study of membrane-active agents in general. Finally, in the case of alamethicin, the relation between peptide incorporation in the membrane and aggregation suggests a simple explanation for channel gating, as will be presented under Discussion.

Materials and Methods

1,2-Dimyristoyl-*sn*-glycero-3-phosphocholine (DMPC) was a Fluka puriss. product. 1,2-Dioleoyl-*sn*-glycero-3-phosphocholine (DOPC) was obtained from Avanti Polar Lipids (Birmingham, AL). Alamethicin was prepared as described below. All solutions were prepared from quartz-distilled water, buffered with 10 mM Tris titrated to pH 7.4 with HCl, at room temperature. In addition, they contained 50 μM EDTA.

Stock solutions of alamethicin were prepared in CH_3OH/H_2O (1:3) at a concentration of 1–1.5 mg/mL and stored at 4 °C for a few weeks. The concentration of each stock solution was determined by CD after dilution with pure methanol. The mean residue ellipticity determined for our preparation of alamethicin was $[\theta]_{220} = -12750$ deg cm^2 dmol^{-1} in methanol at 20 °C. Usually a solution of alamethicin with a 10 times lower concentration was prepared in the appropriate buffer for titration experiments. The methanol

† This work was supported by Grant 3.490.83 from the Swiss National Science Foundation.

[1] Abbreviations: CD, circular dichroism; DMPC, 1,2-dimyristoyl-*sn*-glycero-3-phosphocholine; DOPC, 1,2-dioleoyl-*sn*-glycero-3-phosphocholine; NMR, nuclear magnetic resonance; HPLC, high-pressure liquid chromatography; EDTA, ethylenediaminetetraacetic acid; TLC, thin-layer chromatography; Tris, tris(hydroxymethyl)aminomethane.

0006-2960/87/0426-2751$01.50/0

content of the solutions used for titrations never exceeded 0.6%.

Stock solutions of small unilamellar vesicles were prepared on the day of the experiment by sonicating a lipid dispersion (~5 mM) with a titanium tip sonifier for about 30 min. The temperature was kept around 25 °C for DOPC and around 32 °C for DMPC with the help of a thermostating jacket. The optically clear solutions so obtained were then centrifuged for 10 min in an Eppendorf centrifuge in order to remove metallic titanium. In the case of DOPC vesicles, all the operations were carried out under a flow of nitrogen or argon, using buffer saturated with nitrogen beforehand. The lipid concentration was determined by phosphate analysis (Ames & Dubin, 1960) with an accuracy of ±5%.

CD measurements were carried out on an extensively modified version (Baechinger et al., 1979) of a Cary 61 instrument that was periodically calibrated with a batch of D-(+)-10-camphorsulfonic acid of known chemical and optical purity, on the basis of a molar ellipticity $[\theta]_{290}$ = 8220 deg cm^2 dmol^{-1} (De Tar, 1969). Fluorescence experiments were done on a Schoeffel RRS 1000 recording fluorometer. The temperature was controlled with a Lauda thermostat Type TUK 30 D and measured at the end of each experiment with a platinum resistance thermometer inserted in the central part of the optical cell. ^{1}H NMR spectra were measured at Ciba-Geigy AG, Basel, with a Bruker WM 400 spectrometer operating in the Fourier transform mode. Chemical shifts at 298 K were determined with respect to the internal reference of the instrument, which was calibrated against tetramethylsilane.

Measurements of conductance across planar lipid membranes were carried out with equipment designed according to Schindler and Feher (1976). Membranes were formed on Teflon sandwich septa by painting or by apposition of two monolayers. Hole diameters were either 0.1 or 1 mm.

Titrations were done in thermostated fused silica cuvettes of 1- (CD) or 0.4-cm (fluorescence) path length, usually by microliter additions of a concentrated vesicle solution to an alamethicin solution. Alamethicin was also present in the vesicle solution in order to keep its concentration constant in the course of a titration experiment. The contribution of lipid vesicles to either CD or fluorescence was independently determined and subtracted from the titration data. Base line drift in a CD experiment was checked by monitoring the signal at 260 nm, where alamethicin shows no significant contribution.

Preparation and Characterization of Alamethicin. Alamethicin was purified from chloroform extracts of about 10-L culture medium of *T. viride* NRRL 3199 by a modification of the procedure described by Irmscher and Jung (1977). The crude extract was generously donated by Prof. G. Jung, Institute of Organic Chemistry, University of Tübingen, Tübingen, FRG.

An alamethicin-rich fraction was precipitated from a methanolic solution of the crude extract by addition of an excess of diethyl ether (10 times by volume). The precipitate was redissolved in methanol and chromatographed in 2-mL portions on a Sephadex LH 20 column (3 cm × 60 cm) eluted with methanol. Fractions were assayed by TLC, and the alamethicin-containing ones were pooled and then rechromatographed through the same column. This yielded a mixture of several alamethicin components that was further fractionated by chromatography on a silica gel H column (1.8 cm × 24 cm) eluted with $CHCl_3/CH_3OH/H_2O$ (65:25:4) (Melling & McMullen, 1975). Satisfactory separation was obtained by loading 15–20-mg batches.

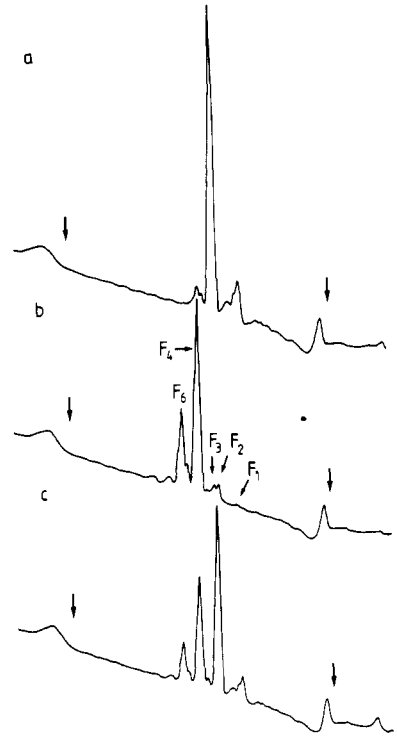

FIGURE 1: Comparison by HPLC of the alamethicin used in this study (a) with the Upjohn standard alamethicin (b). The trace in (c) represents a mixture of the two. Column Nucleosil 5-C-18 (Macherey & Nagel, Düren, FRG); absorption detection at 214 nm; flow rate 1 mL/min. Mobile phases A and B were identical with those described by Balasubramanian et al. (1981), but elution was obtained with a gradient from 35% to 55% mobile phase B in 20 min. The start and end of the gradient are indicated by arrows on each trace. Some of the relevant components of the Upjohn sample are indicated with the nomenclature used by Balasubramanian et al. (1981).

The purified material used in this study was compared with an original sample of alamethicin kindly donated by The Upjohn Co. (Kalamazoo, MI) on HPLC equipment using solvents and conditions similar to those reported in the literature (Balasubramanian et al., 1981; Gisin et al., 1981). As shown in Figure 1, the principal component of our material had chromatographic properties very similar to those of two minor fractions of the Upjohn sample, which are referred to as F_2 and F_3 by Balasubramanian et al. (1981). Insufficient resolution in our HPLC prevented a more detailed comparison. The major fraction of the Upjohn alamethicin, F_4, was only present in small quantities in our preparation and, together with other minor components, accounted for about 15% of the composition. A 400-MHz ^{1}H NMR of our sample in CD_3OD was in very good agreement with that reported by Banerjee et al. (1983), with the exception of small chemical shift differences found for signals assigned to residues of the C-terminal portion of the peptide. The signals of an unassigned valine residue, observed for the Upjohn sample and reported to disappear in the spectrum of the purified F_4 fraction (Banerjee et al., 1983), were also absent in our preparation.

Following previous observations (Melling & McMullen, 1975; König & Aydin, 1980; Jung et al., 1981) we conclude that the chemical structure of our major component differs from that reported by Rinehart et al. (1977) in the substitution of a glutamine for glutamic acid at position 18 in the sequence. This is strongly supported by potentiometric titration of the peptide in a H_2O/CH_3OH mixture (3:1 by volume), where only 0.05 equiv of NaOH/mol of peptide was used with our sample, in contrast to the 1.01 required by the Upjohn alamethicin.

The electrical conductivity induced by our alamethicin on black lipid membranes made of DOPC in *n*-decane (1% w/v) was found to be consistent with that reported in the literature (Eisenberg et al., 1973; Boheim & Kolb, 1978; Hanke et al., 1983). Well-resolved single-pore states were seen at low alamethicin concentration. At higher concentrations, the potential-dependent rise of the conductance was proportional to $\exp(V/V_0)$, with $V_0 = 4.5 \pm 0.3$ mV as compared to a literature value of 4.1 ± 0.1 mV (Boheim & Kolb, 1978) for the same lipid at room temperature. By use of soybean lecithin instead of DOPC, the alamethicin conductance was strongly asymmetric, being induced only by potentials that were positive on the side of added alamethicin.

Theoretical Model. Interpretation of our data calls for a model that comprises the following features: (1) a membrane–water partition equilibrium of the (monomeric) peptide; (2) aggregation of the peptide within the membrane; (3) peptide–peptide interactions at a high degree of incorporation in the membrane, accounted for by appropriate activity coefficients for the various states of the peptide in the bilayer phase. Such a model has been presented recently (Schwarz et al., 1986). Here we shall briefly give its essentials.

Let $c_P = c_f + c_a$ be the total molar concentration of peptide, where c_f is the free (aqueous) concentration and c_a is the lipid-associated part. A more convenient measure of the peptide concentration in the membrane is given by dividing c_a by the total concentration of lipid c_L, which gives the "extent of incorporation" $r = c_a/c_L$. (Volume corrections in the presence of lipids never exceeded 0.5% and were neglected.) Assuming a two-state model, the difference of optical signals per mean residue, in the presence and absence of lipids, F is proportional to r:

$$F = F_\infty r c_L / c_P \tag{1}$$

where F_∞ is the value of F for the peptide incorporated in the bilayer. Provided there is no aggregation in the aqueous phase, the extent of incorporation r_1 of monomeric peptide is expressed as

$$\alpha_1 r_1 = \Gamma_1 c_f \tag{2}$$

with an appropriate partition coefficient Γ_1 and an activity coefficient α_1 correcting for peptide–peptide interactions in the lipid bilayer. Generally, for a given monomeric or aggregate component such an activity coefficient can be described in terms of a purely entropic contribution, α_S, together with an enthalpic one, α_H:

$$\alpha = \alpha_S \alpha_H \tag{3a}$$

$$\alpha_S = (1 + 2r)^z \tag{3b}$$

$$\alpha_H = \exp[-[1 - (1 + 2r)^{-2}]\Delta H/RT] \tag{3c}$$

The entropic part is derived on the basis that an insertion site can contribute to the solvation entropy only if surrounded by a minimum number of lipid molecules (related to the parameter z). The enthalpic part is of the Bragg–Williams approximation type (Hill, 1960), ΔH being an effective mixing enthalpy. The factor of 2 in the expression $1 + 2r$ relates to the fact that the peptide is thought to span the membrane [see Schwarz et al. (1986) for more details].

In addition to these corrections for thermodynamically nonideal behavior, the model includes peptide aggregation in the membrane. An isodesmic model is chosen; i.e., the equilibrium constant K for adding a monomer to an aggregate is independent of aggregate size. For the activity coefficients of the various aggregates, constant increments of z and ΔH are assumed when one goes from an aggregate of size i to one of size $i + 1$; in other words, $\alpha_{i+1} = \alpha\alpha_i$ with a constant factor α as given by eq 3. For aggregates of size i we then have

$$r_i = s^{i-1} r_1 \tag{4}$$

where $s = (\alpha_1/\alpha)Kr_1 = \Gamma_1 K c_f/\alpha$. No aggregation is considered in the aqueous phase, so eq 2 is applicable. The total extent of incorporation into the bilayer is finally described by a set of formulas:

$$Kr = s/(1 - s)^2 \qquad s = (c_f/c_f^*)/\alpha \qquad c_f^* = (\Gamma_1 K)^{-1} \tag{5}$$

c_f^* is the "critical concentration" in the water phase; it is linearly related, via the partition coefficient Γ_1, to the corresponding critical membranous concentration $r^* = 1/K$.

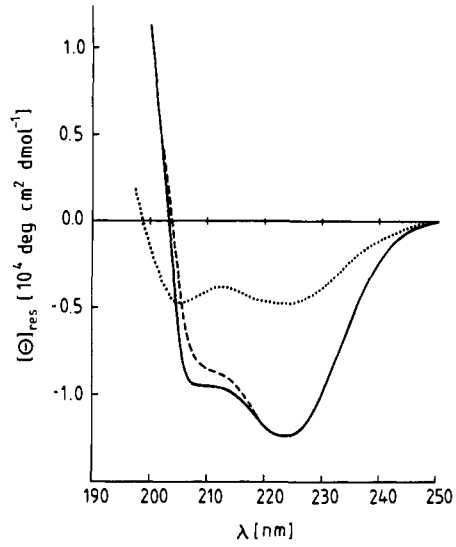

FIGURE 2: CD spectra of alamethicin in aqueous solution (dotted line) and in the presence of 1.9 mM DMPC vesicles (solid line) or 1.7 mM DOPC vesicles (broken line). The solutions were buffered with 10 mM Tris-HCl, pH 7.4, and 10 mM NaCl; the alamethicin concentration was 86 μM for the spectrum in the pure aqueous medium and 68 μM for the other two cases.

RESULTS

Circular Dichroism. The circular dichroic signal of aqueous alamethicin changes considerably upon addition of small unilamellar vesicles of either DMPC or DOPC (Figure 2). The spectral difference is particularly large around 224 nm. Thus, we have chosen the signal at this wavelength for monitoring lipid–alamethicin interactions.

For a quantitative interpretation of the data, we first had to rule out several possible artifacts known to complicate optical work with lipid dispersions and vesicle solutions: Light scattering and absorption flattening generally decrease the photometric readings, while anisotropic scattering of circularly polarized light may distort CD spectra in unpredictable ways. These effects are thought to be minimized by the use of small unilamellar vesicles (Mao & Wallace, 1982). The vesicles used in our study met this criterion, being extensively sonified and having average diameters in the range of 200–300 Å, as determined by negative-stain electron microscopy. However, alamethicin is known to induce vesicle fusion (Lau & Chan, 1974), and indeed, under the electron microscope our vesicles appeared to increase in size upon interaction with the peptide. At total lipid to peptide ratios of 50–100, average vesicle diameters were approximately doubled, whereas at high peptide content, smaller particles also appeared. These may represent deformed or fragmented vesicles or other bilayer structures. Although we cannot be sure that vesicles remain intact at the very high peptide densities reached, the rever-

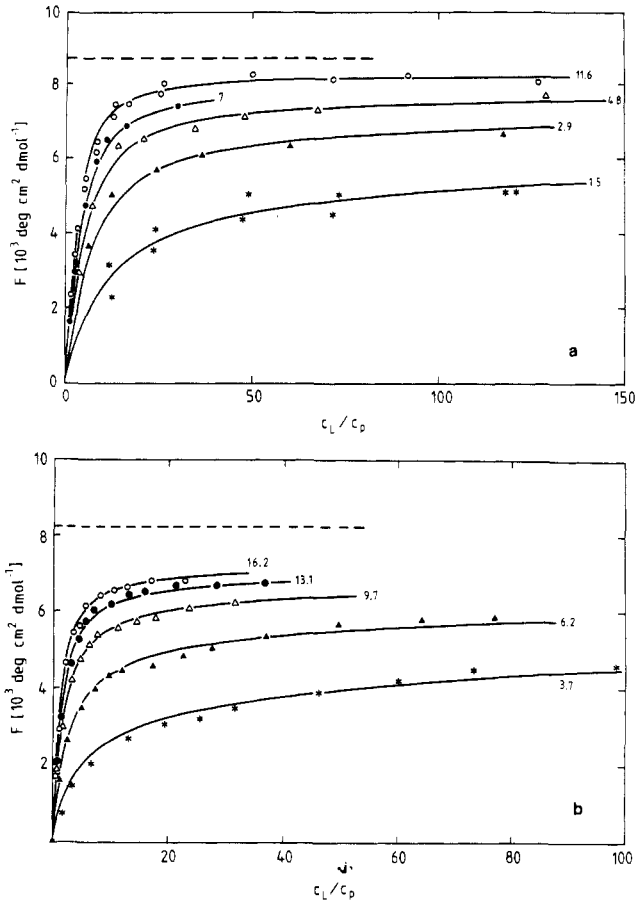

FIGURE 3: Increase of the negative mean residue ellipticity at 224 nm, F, of alamethicin (at concentrations c_P as indicated in micromolar) upon titration with lipid vesicles. (a) DMPC vesicles at 31 °C, in the absence of added NaCl; (b) DOPC vesicles at 21 °C, in the absence of added NaCl. Solid lines are fitted according to our theoretical model, with values of the parameters as indicated in Table I.

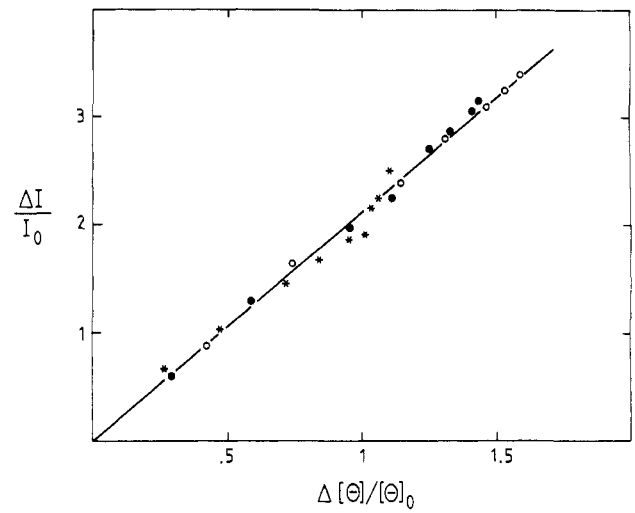

FIGURE 4: Proportionality of signals obtained with fluorescence and CD techniques. The difference of optical signals obtained in the presence and in the absence of lipids, divided by the signal of the pure aqueous peptide, is plotted for both spectroscopic methods. Each entry is taken at equal values of lipid and peptide concentration: c_P = 1.5 (*), 3 (●), and 6 μM (○). Data points lie on a straight line through the origin, which demonstrates equivalence of fluorescence and CD results.

sibility of our data (see below) effectively excludes micellization or similar phenomena that would only slowly revert as titrations are continued to high lipid concentrations. In support of this conclusion, Banerjee et al. (1985) have shown by NMR that DMPC lipids remain in the bilayer configuration at peptide to lipid ratios as high as 1:2. (Similar reversibility arguments suggest that the interaction of peptide and lipids is not strongly affected by vesicle fusion.)

In order to exclude light scattering artifacts, we performed some control experiments using two water-soluble proteins, lysozyme and bovine serum albumin. The latter is known to interact with lipids at low pH (Sweet & Zull, 1970) but not at neutral pH as is the case here. The CD signals of these proteins remained unchanged upon addition of lipids up to the maximal concentration used in our study, in the absence as well as in the presence of alamethicin.

The contribution of absorption flattening was estimated from the theory of Gordon and Holzwarth (1971) and found to be negligible under our experimental conditions. This is essentially due to the relatively low absorption coefficient of alamethicin at 224 nm ($<10^4$ M^{-1} cm^{-1}).

Reversibility of peptide–lipid association was checked by performing titration experiments in both directions, either by adding vesicles to an alamethicin solution (standard procedure) or by adding increasing amounts of alamethicin to a vesicle solution (controls). The results were identical in both cases. Also, the signal obtained at low alamethicin and lipid concentrations was reproduced by diluting samples of higher concentrations. These observations confirm that the investigated process can be regarded as a thermodynamic equilibrium.

As an example of the original data, Figure 3 shows the increment of the absolute ellipticity per mean residue at 224 nm, F, as a function of the total lipid to peptide ratio c_L/c_P, obtained with vesicles of DOPC as well as DMPC in the liquid-crystalline state. A characteristic feature of these curves is the marked dependence of the apparent plateaus on alamethicin concentration. In the concentration range accessible to our experimental method, the effect is more clearly evident in the case of DOPC, but is nevertheless visible for DMPC, too.

Evaluation and interpretation of these data rely on the assumption that the measured signal can be taken to be proportional to the relative amount of incorporated alamethicin. From an experimental point of view, it would be desirable to check this two-state assumption by an independent method detecting peptide–lipid interaction. Control experiments have therefore been done that exploited the intrinsic fluorescence of the alamethicin molecule.

Fluorescence. Alamethicin carries at its carboxyl terminus an amino alcohol residue, phenylalaninol, endowing the peptide with intrinsic fluorescence. Unfortunately, this phenyl group fluorescence is not really apt for standard investigations because of the small quantum yield. In addition, at the low concentrations of interest in this study, the emission at 285 nm is totally buried under the Raman scattering peak of water, if the normal excitation at 260 nm is chosen. We therefore worked under rather extreme conditions, exciting at 220 nm (and observing the emission at 285 nm). In order to compensate for the weak lamp intensity at such a short wavelength, bandwidths of 6.6 nm had to be tolerated.

The alamethicin fluorescence increased strongly upon addition of lipid vesicles. Titrations could be performed in the same way as for the CD measurements but were limited to moderate alamethicin and lipid concentrations in order to avoid light scattering and inner filter problems. The titration curves were strictly proportional to those obtained by the CD technique. This result is demonstrated in Figure 4 by plotting the fluorescence vs. the CD signal, at equal values of c_L and c_P. Obviously, the data points fall on a straight line through the

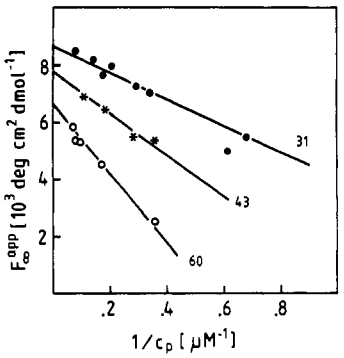

FIGURE 5: Extrapolation of apparent limiting values of F, F_∞^{app}, obtained from individual titration curves as shown in Figure 3. The ordinate intercept for values of $1/c_P$ going to 0 determines F_∞. Data are for DMPC vesicles at 31 (●), 43 (*), and 60 °C (○).

Table I: Thermodynamic Parameters for Alamethicin Incorporation in Bilayers

lipid	temp (°C)	F_∞ (deg cm^2 dmol^{-1})	c_f^* (μM)	z
DMPC, no NaCl	31[a]	8700	0.75	8.5
	43	7800	1.45	5.5
	60	6700	2.9	4.2
lipid	[NaCl] (M)	F_∞ (deg cm^2 dmol^{-1})	c_f^* (μM)	z
DOPC (21 °C)	0[b]	8200	2.7	2.4
	0.05	8600	2.3	2.1
	0.1	8800	2.1	2.7
	0.2	9200	1.65	3.1
	0.5	9800	0.9	3.2

[a] No dependence on NaCl concentration observed in the range 0–0.1 M NaCl at this temperature. [b] No dependence on temperature observed in the range 11–50 °C.

origin. (Except for the very last point, the apparent absorbance at 220 nm and a 0.4-cm light path was always below 0.1.)

Thus, the two different spectroscopic techniques, CD (which is related to the backbone conformation of the whole molecule) and phenylalaninol fluorescence (reporting the environment of one end of the molecule), cannot resolve more than two distinct states: aqueous and lipid-associated alamethicin, respectively.

Isotherms. For a quantitative interpretation of our data we need F_∞, the signal of the lipid-associated peptide. This value is particularly difficult to obtain, in our case, due to the concentration dependence of the apparent plateaus seen in Figure 3. By means of double-reciprocal plots we can extract only apparent limiting values F_∞^{app}, which still depend on c_P. However, replotting these F_∞^{app} vs. $1/c_P$ allows us to extrapolate the corect value of F_∞ (see Figure 5). A detailed justification of this procedure has been given elsewhere (Schwarz et al., 1986).

F_∞ values are reported in Table I for a variety of conditions, using both DMPC and DOPC. Once determined, these were used to extract the amounts of aqueous alamethicin and of lipid-associated alamethicin from the raw data and to construct isotherms where the extent of association, r, is plotted vs. the free (aqueous) concentration, c_f (see Figure 6). Under given conditions of temperature and salt, all data fall on one single isotherm, as they should according to fundamental principles (Schwarz et al., 1986). This criterion can be considered as an additional check of consistency for the determination of F_∞.

Looking at Figure 6, the most striking feature is the initial "lag" of the isotherms. They start very flat and above a

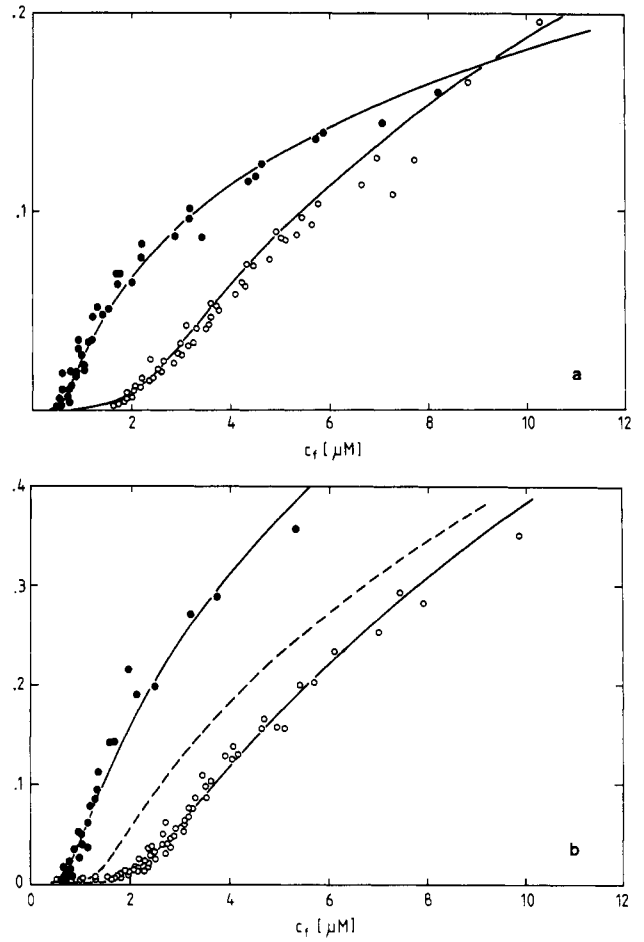

FIGURE 6: Plot of degree of incorporation of alamethicin, r (incorporated peptide per lipid), vs. free aqueous concentration: (a) DMPC at 31 (●) and 60 °C (○) in pure buffer; (b) DOPC at 21 °C in the absence of NaCl (○) and with 0.5 M NaCl added (●). The solid lines are fits obtained by using the parameters given in Table I. The dashed line in (b) is a corresponding fit for DOPC vesicles in the presence of 0.2 M NaCl (data are not shown for the sake of clarity).

threshold concentration suddenly bend upward. Operationally, an apparent critical concentration c_f^0 may be defined in a model-independent way by extrapolating the steep part of the isotherms back to the abscissa. In our model of alamethicin aggregation (see Theoretical Model) a theoretical parameter, c_f^*, appears. The latter turns out to be always slightly larger than the c_f^0 obtained by simple inspection of the experimental curves.

Dependence on Type of Lipid, Ionic Strength, and Temperature. Values of c_f^* (obtained from curve fitting as discussed below) are given in Table I for various experimental conditions. These critical concentrations are seen to depend on the type of lipid used, being larger for the unsaturated species, DOPC. For this lipid, titrations were performed in pure buffer at 11, 21, 36, and 50 °C. Apart from an apparent decrease in the CD signals at high temperature for the highest alamethicin concentrations only (which was attributed to vesicle aggregation and precipitation), no significant temperature effect could be detected for this system. The addition of NaCl to the buffer, on the other hand, gave rise to an increase in the limiting signal F_∞ and to a downward shift of the critical concentration. In the presence of 0.5 M NaCl, the largest concentration investigated, the critical concentration is reduced to one-third the value it had in buffer alone.

In the case of DMPC, titrations were performed at 31 °C, well above the gel–liquid-crystalline phase transition of the lipid, in pure buffer and with solutions containing 10, 50, and

100 mM NaCl, respectively. We were unable to measure at higher salt concentrations with this lipid, due to excessive vesicle aggregation which led to a visible increase of the turbidity of the samples and a slow decrease of the CD signal with time. In contrast to the case of DOPC, temperature dependence is observed with DMPC: F_∞ increases, the critical concentration shifts upward, and the form of the isotherm changes upon going from 31 to 43 and 60 °C in pure buffer. (Note that no phase transition is known to occur for this lipid in that temperature range.)

Discussion

From our CD results at 224 nm and assuming a contribution of −29 500 deg cm^2 dmol^{-1} for an average, 10-residue α-helix (Chen et al., 1974), we estimate a conformation with about 50% α-helix for alamethicin in DOPC at 0.5 M NaCl, a condition where the largest CD signal is obtained. A slightly higher amount of ordered structure is obtained if the signal is interpreted as a superposition of α and β conformations. This estimate agrees well with that obtained in another study (Cascio & Wallace, 1985), although the molar ellipticity reported by these authors for alamethicin incorporated in DMPC vesicles is considerably higher than that determined by us for the same system. The difference may depend on the procedure used by the above authors in the determination of alamethicin concentration. This is supported by a comparison of the values of molar ellipticity of alamethicin in pure methanol, which differ similarly in the two studies.

A more detailed conformational analysis, which should consider the full CD spectrum and discuss possible artifacts arising at shorter wavelengths, is beyond the scope of the present investigation. We can conclude, however, that the membrane conformation of alamethicin depends slightly on the type of lipid (cf. Figure 2 and Table I) and on the conditions of ionic strength and temperature: the CD signal, F_∞, increases upon adding NaCl, for DOPC, and it decreases on raising the temperature, for DMPC (cf. Table I).

Further information can be obtained from the association isotherms (cf. Figure 6). Very high ratios of peptide to lipid, r, can be reached without apparent saturation: the last data point in Figure 6 is $r = \sim 0.35$, corresponding to less than three lipid molecules per peptide. Taken together with the substantial conformational change mentioned above, this appears to argue strongly in favor of the peptide incorporating into the membrane rather than merely binding to the interface. This point has been discussed in more detail previously (Schwarz et al., 1986). As already mentioned, incorporation is also consistent with direct evidence from cross-linking studies (Latorre et al., 1981). We believe that the results of one recent NMR study (Banerjee et al., 1985), where no perturbation of the lipid chains could be found in the presence of alamethicin, can be rationalized by assuming a conformation optimized for minimal perturbation of the hydrophobic core of the bilayer. This might be even more true under conditions of extensive clustering, as can be inferred for that study. We have therefore decided to interpret our data in terms of a water/membrane partition equilibrium where the lipid takes the part of a solvent. In contrast to using binding models, we do not assume the existence of a given number of saturable sites. In view of the very high density of alamethicin attained in the bilayer, this "solvation" process can clearly not be considered to be thermodynamically ideal. We therefore include activity corrections in our model.

Partitioning and Aggregation. The properties of the alamethicin/lipid/water system can best be visualized by looking at Figure 6, where the extent of incorporation, r, is plotted as a function of the aqueous concentration, c_f. As compared to simple ideal partitioning (which would yield a straight line in such a representation), the existence of a critical concentration (cf. Results) immediately suggests the presence of some sort of aggregation phenomenon. If aggregation occurred only in the water but not in the bilayer phase, the opposite course of the isotherms should be expected: a steep rise at the origin, followed by a pronounced flattening around the critical concentration. Thus, the shape of our isotherms must indicate aggregation of the peptide in the membranes. Implication of the lipid phase is also evident from the dependence of c_f^* on the type of lipid used in the titrations. From this reasoning alone, nothing can be said about the situation in the aqueous phase. However, we could not obtain any spectroscopic evidence of alamethicin aggregation in water within the concentration range used in this study (up to 16 μM). Some indication of aggregation could be detected at higher concentrations (>30 μM), in particular for solutions containing 0.5 M NaCl. This is in agreement with findings of Jung et al. (1975), who report evidence of aggregation above 100 μM for alamethicin in water.

For the quantitative treatment of our data, we therefore assume that alamethicin is monomeric in the water phase. At first glance, this might seem to disagree with the results of Mc Mullen and Stirrup (1971), who postulated a critical micelle concentration for alamethicin of 2.5 μM from interfacial tension measurements at a water–decane interface. However, their data can equally well be interpreted by assuming nonideal repulsive interactions in the interface. In any case, allowing for alamethicin aggregation in the water phase would not change any qualitative aspects of the discussion to be given below but would only increase the number of parameters needed, which at this time is not warranted by the experimental data.

We consider a partition equilibrium of peptide monomers between the water and lipid bilayer with a partition coefficient as defined under Materials and Methods. From the lag of the isotherm it can be concluded that the monomer has a comparatively moderate affinity to the lipid phase, Γ_1 being of the order of 10^3 M^{-1} for DOPC in pure buffer. This Γ_1 refers to the peptide to lipid ratio as the concentration variable for the lipid phase (see eq 2). The ordinary partition coefficient, defined as a ratio of molar concentrations, is of the order of 10^3.

As the aqueous concentration of alamethicin is gradually increased, the total extent of incorporation, r, slowly goes up until a critical concentration is reached, where massive internal aggregation apparently starts to develop. In the theoretical model that we use to interpret our data, we have chosen the simplest possible approach to describe aggregation in the membrane, with the same equilibrium constant K to describe each aggregation step independent of the aggregate size (isodesmic model). A more general version of the same model has been given previously (Schwarz et al., 1986), and other models can be conceived easily. It turns out, however, that the experimental data do not allow us to distinguish between the various models. In this situation, we think the simplest choice should be made. If ideal behavior were maintained in the presence of aggregation, the isotherm would sharply rise to infinity when approaching c_f^*. Experimentally, however, the incorporation curves are seen to continue beyond c_f^* and to flatten somewhat at high c_f (Figure 6). Clearly, further insertion of alamethicin is rendered less favorable once a high density of the peptide is reached in the membrane. Thermodynamically, the situation can be adequately described by

introducing activity coefficients such as those given by eq 3 above.

With our approach the whole set of data can be fitted in a very satisfactory way. Examples are shown in Figures 3 and 6, where the same sets of parameters are used to fit two different representations of the data. In a similar way, incorporation isotherms have been measured and the relevant parameters evaluated under a variety of conditions, as shown in Table I. In this compilation, F_∞ is a purely empirical parameter, whereas c_f^*, Γ_1, and K depend on the particular model used.

In order to separate the partition coefficient Γ_1 and the aggregation constant K, which together define the critical concentration c_f^* according to eq 5, sufficiently accurate data are needed in the low c_f range of the isotherm, where monomer incorporation predominates. Unfortunately, this range is not readily accessible by our experimental techniques. The critical concentrations are rather small (generally 2 μM or less). At even lower alamethicin concentrations the poor signal to noise ratio usually does not allow a satisfactory evaluation of data. Only in our most favorable case, namely, DOPC at 21 °C in pure buffer, can we give a reasonable estimate of the partition coefficient, $\Gamma_1 \approx 500\ M^{-1}$ [cf. above; a slightly larger value has been given previously (Schwarz et al., 1986) on the basis of a modified theoretical model]. Otherwise, merely the product $\Gamma_1 K = (c_f^*)^{-1}$ can be given with sufficient confidence. (For the fitted curves in Figures 3 and 6, values of K of about 10^3 have been chosen.)

A further comment is appropriate concerning the assumption of two optically distinguishable states. From the data in Table I and eq 4 and 5 one may easily calculate that the aggregated peptide largely prevails in the membrane under our experimental conditions. The spectroscopic signals (including the F_∞ values) therefore refer essentially to this species. The question remains open whether the monomeric peptide might adopt a slightly different conformation in the bilayer as compared to alamethicin in aggregates.

DMPC Vesicles. Titrations have been performed at 31 °C (well above the gel–liquid-crystalline phase transition of the lipid), in pure buffer and with solutions containing up to 0.1 M NaCl. The experimental curves remained virtually superimposable, independent of the amount of NaCl present. If there is a dependence on ionic strength in this system, it is too small to be detected in the limited range accessible to our study. From an experimental point of view, since c_f^* is already very small in the absence of NaCl, it would clearly be difficult to assess a small downward shift of this parameter (which would mainly show up in experiments conducted at extremely low alamethicin concentration).

On the other hand, effects of temperature are obvious: the decrease in F_∞ indicates a less ordered conformation of the peptide at higher temperature, and the critical concentration shifts upward. Parallel to it, the shape of the isotherms changes: the flattening at high c_f, which is very marked at 31 °C, is strongly reduced at 43 (not shown) and 60 °C (Figure 6). This change of shape is more dramatic between 31 and 43 °C than between the latter temperature and 60 °C and cannot be explained by the enthalpic part of the activity coefficient alone, at least if one excludes strong variations of ΔH with temperature. We tend to interpret the temperature dependence in the case of DMPC as a vestige of the lipid phase transition which, for the pure lipid, occurs at about 23 °C. Some workers have observed that the phase transition shifts to lower temperatures in the presence of alamethicin (Das & Balaram, 1984) whereas others have found it to remain at the transition temperature of the pure lipid (Lau & Chan, 1974). In any case, it appears that this transition is considerably broadened upon addition of alamethicin. Changes in the geometrical arrangement of the lipids may therefore significantly influence the lipid–peptide interaction even at temperatures relatively far from the midpoint of transition.

With these considerations in mind, we prefer to model the high c_f behavior of the isotherms with the entropic part of the activity coefficient alone, letting z vary with temperature. This parameter then decreases from about 7.5 at 31 °C to a value of 4 at 60 °C (Table I). These figures would be somewhat decreased if a negative ΔH were introduced in an additional α_H contribution.

DOPC Vesicles. No temperature dependence could be detected in this system. This is in striking contrast to the situation with DMPC and corroborates the interpretation given above for the latter case. The activity coefficients for DOPC thus only contain the entropic contribution, ΔH being negligible, with a z of about 2.4 independent of the temperature.

A strong salt dependence is evident in the DOPC/alamethicin system. The most dramatic effect is the shift of the critical concentration to low values as the ionic strength is raised. Again, from our data, we cannot ascertain to what extent this is due to an increase in the partition coefficient (conceivably by some "salting out" effect) or to an increase in the aggregation constant.

Anyway, we recall that our preparation of alamethicin is predominantly in the nonionizable form. This excludes counterion screening of a repulsive charge cluster in the aggregate as an explanation of the observed salt effect.

Voltage-Gating Mechanism. As already pointed out in a previous paper (Schwarz et al., 1986), our findings on the incorporation and aggregation of alamethicin in lipid bilayers could provide a straightforward explanation of the voltage gating of alamethicin pores. The proposed mechanism does not require particular conformational changes (Fox & Richards, 1982), a flip-flop of peptides in the membrane (Boheim et al., 1983), or an expulsion of monomers from the center of aggregates (Mathew & Balaram, 1983b). It is simply based on elementary thermodynamic concepts related to the water–membrane partitioning coupled with internal aggregation. In a recent theoretical study on channel kinetics a similar mechanism has been alluded to (Bruner, 1985).

Alamethicin has been shown to have a dipole moment μ of the order of 70 D in lipophilic solvents (Schwarz & Savko, 1982; Yantorno et al., 1982) and is known to incorporate into the membrane in an asymmetric way (Vodyanoy et al., 1983). Assuming all the peptide is incorporated with its dipole moment oriented parallel to the direction of the electric field of strength E in the membrane, there is a contribution of $-\mu E$ to the potential energy of each molecule. Therefore, the higher E is, the more favorable it will be for the peptide to enter the bilayer phase. The partition coefficient will increase by the Boltzmann factor $\exp(\mu E/kT)$. According to eq 4, the number of aggregates of size i then rises by the ith power of that factor (provided K remains constant). The situation is depicted in Figure 7, where all numbers N_i refer to a planar lipid bilayer of 0.01-mm^2 area, representative of conditions encountered in electrical conductance experiments of the single-pore type. Such measurements are typically performed at low alamethicin concentrations (c_f = 0.01 μM has been chosen for Figure 7), far below the range accessible to spectroscopic investigation. Nevertheless, application of our model, together with the parameters evaluated from CD in the micromolar range, allows a quantitative extrapolation.

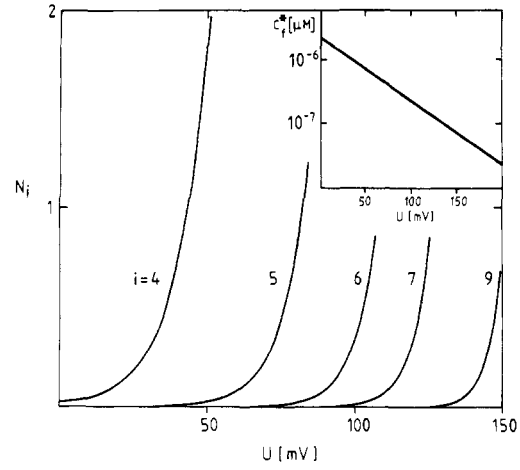

FIGURE 7: Computed number of aggregates of size i (as indicated in the figure) in a planar bilayer of 0.01-mm^2 area as a function of an applied voltage U. The aqueous concentration of alamethicin c_P = 0.01 μM. Parameters used are those for DOPC in 0.1 M NaCl (cf. Table I), assuming a dipole moment of 75 D for the peptide and a bilayer thickness of 2.7 nm (Lewis & Engelman, 1983). (Inset) Calculated decrease of the critical concentration c_f^*, plotted logarithmically vs. U (see text). Conditions and parameters as above.

Under the conditions of Figure 7, the probability of observing a large aggregate would be quite small in the absence of electric fields (e.g., $N_i = 10^{-4}$ for $i = 5$). Application of a potential across the membrane, on the other hand, induces the formation of a sizable number of such aggregates. At least part of them may function as conducting pores.

Current–voltage relationships have been measured by several workers [e.g., Eisenberg et al. (1973) and Latorre and Alvarez (1981)] at slightly higher alamethicin concentrations. They are characterized by a threshold voltage where the conductance starts to rise steeply. In our concept, the existence of such a threshold voltage is naturally related to the existence of a critical concentration. Being inversely proportional to the partition coefficient, Γ_1, the critical concentration, c_f^*, shifts to lower values as Γ_1 increases in the presence of an electric field. With increasing field strength, c_f^* will eventually approach the actual aqueous concentration at which the experiment is done. Incorporation then switches from the flat monomeric branch to the steep aggregate branch of the isotherm (cf. Figure 6). In the inset of Figure 7, the predicted change of c_f^* has been plotted semilogarithmically as a function of applied voltage. The resulting straight line reflects the experimental relationship between aqueous alamethicin concentration and threshold voltage [cf., e.g., Eisenberg et al. (1973)]. Of course, in order to make detailed numerical comparisons, more should be known about the conductance properties of the various aggregates. At the present stage, we find it very encouraging that a simple thermodynamic model of membrane–water partitioning and aggregation can explain so many functional aspects of a voltage-gated membrane pore. More generally, the possibility of introducing a "molecular switch" by means of aggregation in the membrane may be of relevance in other biological processes.

ACKNOWLEDGMENTS

We are grateful to Dr. G. Jung for donating the culture extracts of *T. viride* and to U. Becker for technical suggestions concerning the isolation of alamethicin. We very much appreciate the gift of an original sample of alamethicin from The Upjohn Co. We thank I. Bartoldus for outstanding technical assistance in a delicate stage of this project. We also thank Dr. P. Allegrini for taking the 400-MHz ^{1}H NMR spectra and C. Fauser for performing the electron microscopy.

Registry No. DMPC, 18194-24-6; DOPC, 4235-95-4; alamethicin, 27061-78-5.

REFERENCES

Baechinger, H. P., Eggenberger, H. P., & Haenisch, G. (1979) *Rev. Sci. Instrum. 50*, 1367–1372.

Balasubramanian, T. M., Kendrick, N. C. E., Taylor, M., Marshall, G. R., Hall, J. E., Vodyanoy, I., & Reusser, F. (1981) *J. Am. Chem. Soc. 103*, 6127–6132.

Banerjee, U., Tsui, F. P., Balasubramanian, T. N., Marshall, G. R., & Chan, S. I. (1983) *J. Mol. Biol. 165*, 757–775.

Banerjee, U., Zidovetzki, R., Birge, R. R., & Chan, S. I. (1985) *Biochemistry 24*, 7621–7627.

Boheim, G. (1974) *J. Membr. Biol. 19*, 277–303.

Boheim, G., & Kolb, H. A. (1978) *J. Membr. Biol. 38*, 99–150.

Boheim, G., Hanke, W., & Jung, G. (1983) *Biophys. Struct. Mech. 9*, 181–191.

Bruner, L. J. (1985) *J. Theor. Biol. 117*, 265–276.

Cascio, M., & Wallace, B. A. (1984) *Ann. N.Y. Acad. Sci. 435*, 527–529.

Das, M. K., & Balaram, P. (1984) *J. Biosci. 6*, 337–348.

De Tar, D. F. (1969) *Anal. Chem. 41*, 1406–1408.

Eisenberg, M., Hall, J. E., & Mead, C. A. (1973) *J. Membr. Biol. 14*, 143–176.

Fox, R. O., & Richards, F. M. (1982) *Nature (London) 300*, 325–330.

Gisin, B. F., Davis, D. G., Borowska, Z. K., Hall, J. E., & Kobayashi, S. (1981) *J. Am. Chem. Soc. 103*, 6373–6377.

Gordon, D. J., & Holzwarth, G. (1971) *Arch. Biochem. Biophys. 142*, 481–488.

Gordon, L. G. M., & Haydon, D. A. (1975) *Philos. Trans. R. Soc. London, B 270*, 433–447.

Hall, J. E., Vodyanov, I., Balasubramanian, T. M., & Marshall, G. R. (1984) *Biophys. J. 45*, 233–247.

Hanke, W., Methfessel, C., Wilmsen, H. U., Katz, E., Jung, G., & Boheim, G. (1983) *Biochim. Biophys. Acta 727*, 108–114.

Hill, T. L. (1960) *An Introduction to Statistical Thermodynamics*, Chapter 14, Addison-Wesley, Reading, MA, and London.

Irmscher, G., & Jung, G. (1977) *Eur. J. Biochem. 80*, 165–174.

Jung, G., Dubischar, N., & Leibfritz, D. (1975) *Eur. J. Biochem. 54*, 395–409.

Jung, G., Brückner, H., & Schmitt, H. (1981) in *Structure and Activity of Natural Peptides* (Voelter, W., & Weitzel, G., Eds.) pp 75–114, de Gruyter, Berlin.

König, W. A., & Aydin, M. (1980) in *Peptides 1980, Proceedings of the European Peptide Symposium, 16th, Helsingoer* (Brunfeldt, K., Ed.) pp 711–718, Scriptor, Copenhagen.

Latorre, R., & Alvarez, O. (1981) *Physiol. Rev. 61*, 77–150.

Latorre, R., Miller, C. G., & Quay, S. (1981) *Biophys. J. 36*, 803–809.

Lau, A. L. Y., & Chan, S. I. (1974) *Biochemistry 13*, 4942–4948.

Lewis, B. A., & Engelman, D. M. (1983) *J. Mol. Biol. 166*, 211–217.

Mao, D., & Wallace, B. A. (1984) *Biochemistry 23*, 2667–2673.

Mathew, M. K., & Balaram, P. (1983a) *Mol. Cell. Biochem. 50*, 47–64.

Mathew, M. K., & Balaram, P. (1983b) *FEBS Lett. 157*, 1–5.

Mc Mullen, A. I., & Stirrup, J. A. (1971) *Biochim. Biophys. Acta 241*, 807–814.

Melling, J., & Mc Mullen, A. I. (1975) *ISC-IAMS Proc. Sci. Counc. Jpn. 5*, 446–452.
Nagaraj, R., & Balaram, P. (1981) *Acc. Chem. Res. 14*, 356–362.
Rinehart, K. L., Jr., Cook, J. C., Jr., Meng, H., Olson, K. L., & Pandey, R. C. (1977) *Nature (London) 269*, 832–833.
Schindler, H., & Feher, G. (1976) *Biophys. J. 16*, 1109–1113.
Schwarz, G., & Savko, P. (1982) *Biophys. J. 39*, 211–219.
Schwarz, G., Stankowski, S., & Rizzo, V. (1986) *Biochim. Biophys. Acta 861*, 141–151.
Sweet, C., & Zull, J. E. (1970) *Biochim. Biophys. Acta 219*, 253–262.
Vodyanoy, I., Hall, J. E., & Balasubramanian, T. M. (1983) *Biophys. J. 42*, 71–82.
Yantorno, R., Takashima, S., & Mueller, P. (1982) *Biophys. J. 38*, 105–110.

Modulation of Thrombin-Stimulated Lipid Responses in Cultured Fibroblasts. Evidence for Two Coupling Mechanisms†

Daniel M. Raben,‡ Kathleen Yasuda, and Dennis D. Cunningham*
Department of Microbiology and Molecular Genetics, College of Medicine, University of California, Irvine, California 92717
Received June 6, 1986; Revised Manuscript Received January 8, 1987

ABSTRACT: Treatment of cultured fibroblasts with thrombin results in the stimulation of cell division and lipid metabolism. Proteolytically active α-thrombin rapidly stimulates (a) release of arachidonic acid, (b) generation of inositol phosphates, and (c) increase in cellular diacylglycerol levels. Pretreatment of the fibroblasts with chymotrypsin before α-thrombin prevented the first two responses, (a) and (b), and reduced response c. Treatment of fibroblasts with γ-thrombin, a proteolytic derivative of α-thrombin, produced a response indistinguishable from the α-thrombin treatment when preceded by chymotrypsin. These data support a model, similar to one for platelets [McGowan, E. B., & Detwiler, T. C. (1986) *J. Biol. Chem. 261*, 739–746], that fibroblasts possess two coupling mechanisms for the stimulation of lipid metabolism by thrombin. Similar to platelets, one mechanism, R1, mediates the stimulated release of arachidonic acid and is capable of activating N_i, a GTP-binding protein. R1 is inactivated by chymotrypsin and does not respond to γ-thrombin. The other mechanism, R2, responds to γ-thrombin and is not inactivated by chymotrypsin. In contrast to the mechanisms proposed for platelets, we demonstrate that the phospholipase C responsible for the hydrolysis of phosphoinositides is not activated by R2 but is activated via R1. Importantly, stimulation of either mechanism results in the elevation of cellular diacylglycerol. This indicates that the stimulated elevation of diacylglycerol, or those events dependent upon the elevation of diacylglycerol, is not a reliable indicator for establishing the hydrolysis of phosphoinositides. Furthermore, studies with islet activating protein demonstrate that while a N_i-like protein(s) does (do) not appear to be involved in the stimulated hydrolysis of phosphoinositides, this protein does appear to be involved in at least part of the thrombin-stimulated release of arachidonic acid. A N_i-like protein(s) may be involved in the metabolism of stimuated diacylglycerol.

Addition of catalytically active α-thrombin to certain fibroblast-like cells results in the stimulation of cell division (Chen & Buchanan, 1975; Pohjanpelto, 1978; Carney et al., 1978) and cellular lipid metabolism (Hong & Levine, 1976; Carney et al., 1985; Raben & Cunningham, 1985; Murayama & Ui, 1985). The stimulated lipid metabolism has been strongly implicated in mitogenesis by thrombin (Carney et al., 1985; Raben & Cunningham, 1985) and other growth-promoting agents (Fisher & Mueller, 1968; Cunningham, 1972; Hoffman et al., 1980; Sawyer & Cohen, 1981; Habenicht et al., 1981; Macphee et al., 1984; Berridge et al., 1984; Dawson et al., 1983; Diringer & Friis, 1971; Ristow et al., 1980; Hiu & Harmony, 1980; Hasegawa-Sasaki & Sasaki, 1982; Vicentini & Villereal, 1984). α-Thrombin similarly stimulates lipid metabolism in platelets (Agaroff et al., 1983; Billah & Lapetina, 1982; Kawahara et al., 1980; Sano et al., 1983; Ieyasu et al., 1982; Rittenhouse-Simmons, 1979; Bell & Majerus, 1980; Takai et al., 1982; Lapetina & Cuatrecasas, 1979). Addition of catalytically active α-thrombin to platelets results in a rapid release of inositol phosphates and arachidonic acid and the generation of elevated levels of diacylglycerol (Agaroff et al., 1983; Billah & Lapetina, 1982; Kawahara et al., 1980; Sano et al., 1983; Ieyasu et al., 1982; Rittenhouse-Simmons, 1979; Bell & Majerus, 1980; Takai et al., 1982; Lapetina & Cuatrecasas, 1979). The detailed mechanism by which thrombin-mediated proteolysis is coupled to stimulated lipid metabolism in either fibroblasts or platelets remains to be established.

Detwiler and co-workers have demonstrated that pretreatment of platelets with chymotrypsin, which does not activate platelets, modifies the platelet response to α-thrombin (Tam et al., 1980; McGowan et al., 1983; McGowan & Detwiler, 1986). Interestingly, γ-thrombin, a proteolytic derivative of α-thrombin, elicited platelet responses which were nearly identical with those stimulated by α-thrombin on chymotrypsin-treated platelets (McGowan & Detwiler, 1986). In

† This work was supported by National Institutes of Health Grant CA 12306.
* Correspondence should be addressed to this author.
‡ Present address: Department of Physiology, The Johns Hopkins University School of Medicine, Baltimore, MD 21205.

0006-2960/87/0426-2759$01.50/0